

Ground motion prediction equations for Algeria and surrounding region using site classification based H/V spectral ratio

Nasser Laouami¹ · Abdennasser Slimani¹ · Said Larbes¹

Received: 9 May 2017 / Accepted: 8 January 2018 / Published online: 17 January 2018
© Springer Science+Business Media B.V., part of Springer Nature 2018

Abstract The present work is exclusively based on recorded data provided by the Algerian and the European strong ground-motion database. These data contain 1391 records homogeneously processed with more than 700 records in Algeria and the rest from essentially the Mediterranean region, with distance and magnitude ranging from 5 to 150 km and 3.0 to 7.4 respectively. An emphasis is given to the proposal of appropriate ground motion prediction equation (GMPE) for Algeria and surrounding region considering site classification. This latter is based on the predominant period computed using average horizontal to vertical spectral ratio response (H/V). Four site categories are defined according to Zhao et al. (Bull Seismol Soc Am 96:914–925, 2006) classification scheme. Due to the insufficient number of records for very soft soil, one considers three soil classes for the computation of the empirical predictive spectral ground motion relations: rock, firm and soft. Two cases are studied; the first one considers only local data (52.84% with $3.0 \leq M \leq 6.8$) which serves to illustrate the limits of considering only the country's borders, while in the second case, the regional data is added (47.16% with $M \geq 5.2$) to investigate its influence on the reliability and the robustness of the developed model. A truncation distance criteria is applied with respect to the magnitude and the distance values associated with each data. The obtained results show that (1) the model based on local data overestimates the predicted accelerations for larger magnitude, while the model based on regional data is in good agreement with the last published models; (2) among the four soil classes, the amplitudes and the shapes of the mean H/V spectral ratios are significantly different. Furthermore, the peaks in the period range are reasonably similar to those of site periods defined for each site class by Zhao et al. (2006); (3) the standard

✉ Nasser Laouami
nlaouami@cgs-dz.org
Abdennasser Slimani
aslimani@cgs-dz.org
Said Larbes
slarbes@cgs-dz.org

¹ Centre National de Recherche Appliquée En Génie Parasismique, BP. 252, Rue Kaddour Rahim, Hussein Dey, Algeria

deviation decreases compared to the original rock/soil classification scheme and the obtained mean site coefficients for stiff and soft soil are in good agreement compared to those defined in EC-8 (CEN, Eurocode 8, design of structures for earthquake resistance—part 1: general rules, seismic actions and rules for buildings. EN 1998-1: 2004. Comité Européen de Normalisation, Brussels, 2004); (4) at short distance, the proposed GMPE for Algeria predicts relatively smaller spectral acceleration compared to recent published models possibly due to the differences in the lower magnitude bounds of these models; (5) in addition to the proposed model, this study makes in evidence that Boore et al. (Earthq Spectra 30:1057–1085, 2014) and Akkar et al. (Bull Earthq Eng, 2013. <https://doi.org/10.1007/s10518-013-9461-4>) models are appropriate for the computation of the seismic hazard in Algeria.

Keywords Algerian strong ground motion · GMPE · Site effect · HVSr · Seismic hazard

1 Introduction

The northern Algeria is located in the Africa-Eurasia plate boundary. It is among the most active seismogenic area in the western Mediterranean region. From north to south, northern Algeria is divided into four main structural domains (Bracene et al. 2003). These geological features, related to interplate processes, are: the Tell Atlas or Tell-Rift system, the High Plateaus, the Sahara Atlas or Atlas Mountains system, and the Sahara Platform (Fig. 1a). The seismicity distribution, which is strong to moderate in the northern part, to low in the southern part, is represented by four (04) seismic areas (RPA 2003) (Fig. 1b), seismic zones IIb and III for moderate to strong activity, and I and IIa for weak to moderate ones. During the last three decades, northern Algeria experienced several moderate-to-strong earthquakes; two of them were strongly destructive (Fig. 1a). The 1980 El Asnam earthquake (M7.3), which claimed over 2700 lives and destroyed about 60,000 housings, and Boumerdes May 21 (M6.8) caused considerable damages and claimed over 2300 lives (Laouami et al. 2006; Laouami and Slimani 2013).

Algeria is considered to be part of the active regions with shallow crustal seismicity. In this context, during the last years, several studies regarding the ground motion predictive equations have been developed. These studies account for the important improvement in the understanding of the seismic motion from the earthquake source to the ground surface. Nowadays, several predictive equations, estimated from strong motion recordings, have been proposed around the world (Berge-Thierry et al. 2003; Ambraseys et al. 2005; Zhao et al. 2006; Abrahamson and Silva 2008; Boore and Atkinson 2008; Akkar and Bommer 2010, 2013; Chiou et al. 2010; Boore et al. 2014).

The reduction of the seismic risk in Algeria requires the assessment of the seismic hazard of the whole country and in particular its northern part. However, it is established that the selection of ground motion predictive equations is very crucial and directly controls the uncertainties that affect the final results. The lack, until recently, of strong motion data in Algeria, and the pressing need for studies of seismic hazard in different potentially seismic regions, motivated the use of American and European GMPEs (Sadigh et al. 1997; Ambraseys et al. 2005; Berge-Thierry et al. 2003; Akkar and Bommer 2010) as considered most appropriate to the Algerian tectonic context and some of them have considered a few number of strong motions recorded in Algeria.

However, in a recent study, Gherboudj and Laouami (2013) have carried out a probabilistic seismic hazard assessment of the Algiers city. The region falls within an area of active shallow crustal seismicity, and therefore, the GMPEs of Akkar and Bommer (2010),

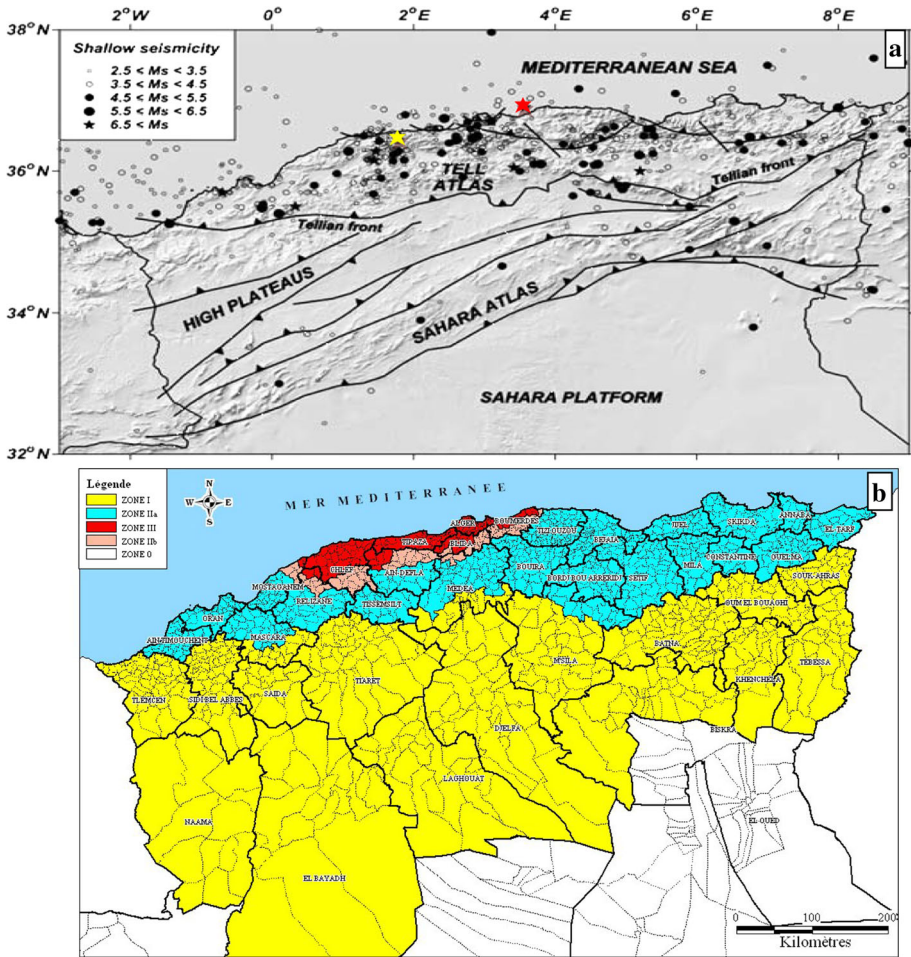


Fig. 1 **a** Seismicity of Algeria since 1700, and regional tectonic setting (Bracene et al. 2003), yellow and red asterisk show respectively the destructive M_s 7.3 El Asnam and M_w 6.8 Boumerdes earthquakes; and **b** Seismic zonation of Algeria (RPA 2003)

Boore and Atkinson (2008), Ambraseys et al. (2005) and Berge-Thierry et al. (2003) are selected to compute the ground motion intensity (PGA, PSA (T)) at the considered site. An equal weight is assigned to each equation within the logic tree framework. The obtained hazard curves reveal a strong epistemic uncertainty due to GMPE’s selection. There is a significant dispersion between the different models, which makes the selection of appropriate GMPEs a very difficult task. Among the parameters that cause this dispersion, one can cite the considered minimum magnitude. Several studies (Frisenda et al. 2005; Massa et al. 2007) pointed out that well calibrated GMPEs, spanning from weak motions to strong motion, are necessary. According to some authors (Atkinson and Boore 2011; Akkar et al. 2013; Boore et al. 2014), as this magnitude value is high, as the model overestimates the predicted accelerations at low magnitude. In this study, one considers a minimum magnitude equal to 3.0.

Otherwise, it is well known that precise site classification is important in determining accurate empirical ground motion prediction relations. In this study, the site condition at a recording station is investigated. Until now, the majority of the strong motion stations in Algeria have limited geotechnical information. In order to evaluate the site amplification, HVSR spectral ratio analysis has been performed over more than 1600 strong motion data. The site classification is based on the computed predominant period. Four site categories are defined according to Zhao et al. (2006) classification scheme.

Finally, this study do not considers the amplitude saturation effect, because near fault strong motion records are very scarce in Algeria and in the surrounding Mediterranean region. Furthermore, due to their complexity, directivity and hanging wall effects strongly affect seismic motion near the fault are not considered in this study. The development and use of this model in the assessment of the seismic hazard in Algeria will reduce the epistemic uncertainties induced by the use, only, of models developed in other sismotectonic contexts.

2 Strong motion data

The lack of strong ground motion data was significantly experienced when elaborating the first Algerian aseismic building code in 1976. It was therefore decided to implement a countrywide accelerometer network. The installation of 335 3-component accelerographs started in 1980, 218 are already installed in the free field and 30 in structures (buildings, dams ...etc.) (Fig. 2). The network was acquired in three stages: (1) following the 1980 El Asnam earthquake, 90 analog SMA-1 accelerographs were installed mainly in the free field, (2) in 1990, 80 SMA-1 analog and 40 SSA-1 digital accelerographs were acquired in order to densify the existing network, with more emphasis on structures (buildings, dams), and (3) 125 Etna digital accelerographs, acquired in 2002–2003.

The installation and the development of an accelerographs network and the collect of instrumental recordings of strong earthquake shaking are crucial for improving the earthquake resistant design of buildings and for understanding earthquake source mechanisms, as well as seismic wave propagation from the source to the site of interest, including local site effects. However, the reliability of such measures requires preconceptions as to classify sites on which the stations are installed. This is usually done in a crude way because of the high cost of geotechnical and geophysical investigations. The main

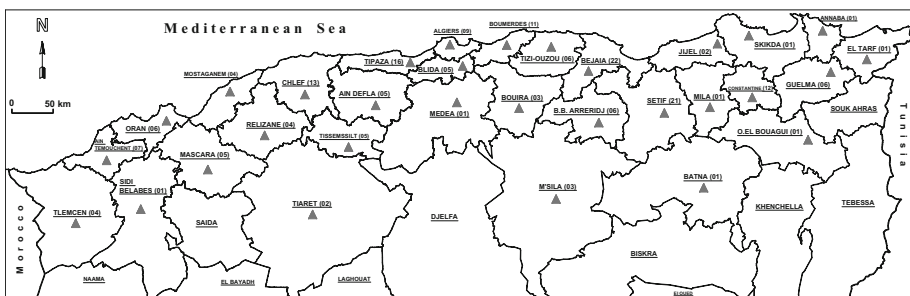


Fig. 2 The national accelerograph network, with the regional administrative limits. The numbers in parentheses next to the filled triangles stand for the number of stations installed in the region (Laouami et al. 2006)

parameter used in the modern code provisions concerning site classification is V_{s30} , i.e. the time averaged shear wave velocity in the upper 30 m of the soil profile. As it is well known, the shear wave velocity profile is rarely available in civil engineering or geotechnical engineering applications because of the cost of the geophysical investigations. In the recent years, it has been shown that NHV (horizontal to vertical spectral ratio from ambient noise) and EHV (from seismic motions) can supply useful information about the resonance properties of the shallow subsoil and represent a cost-effective tool for micro-zoning studies and site classification (Fukushima et al. 2007) and retrieve information on the subsoil seismic layering. The difficulty to have the average shear wave velocity over 30 m, and the fact that V_{s30} does not always capture the predominant period of the site, since it represents only the shallowest portion of the geological profile (Fukushima et al. 2007) has encouraged the development of other site classification schemes. Based on the predominant period via H/V spectral ratios, Zhao et al. (2006) proposed four site categories and classified K-net sites. This classification scheme was also used to categorize the Iranian strong motion network (ISMN) (Ghasemi et al. 2009). Recently Beneldjouzi and Laouami (2015) proposed a site classification based on random field simulation and considering the criteria required by the Algerian seismic code (RPA99). As the latter is being revised, we have used, to classify the recorded data provided by the Algerian and the European strong ground-motion databases, the classification scheme proposed by Zhao et al. (2006).

The development of the strong motion database in Algeria is a fundamental step for any application in the field of earthquake engineering. The main description parameters for each record are magnitude, distance and soil class to describe respectively the source, path and site effects. To date, the Algerian strong motion database contains 96 seismic events (main shock and aftershocks) recorded since El Asnam earthquake 1980 ($M = 7.3$) up to the Algiers earthquake in 2014 ($M = 5.5$). Two periods characterize the evolution of the strong motion database. The first one, 1980–2000, is dominated by analog recordings as analog instruments formed the bulk of the network. The second, 2003–2017, characterized by the development of a new digital network of 125 instruments, made it possible to densify the accelerograph national network and increase the quality and the quantity of the database (more than 1000 accelerograms and more than 95% of digital data). The present Algerian database which contains more than 1000 records including around 735 horizontal components is used to derive the ground motion predictive equation for Algeria. This database contains information on the main predictor variables used in our regression analysis which are the available surface wave magnitude as evaluated by USGS and converted to moment magnitude (Akkar et al. 2013), the hypocentral distance as it allows accounting for both point sources and extended ruptures, also because fault geometries are still unknown for most moderate-sized events in the region, and the soil class allowing a better prediction of the seismic motion in the rock condition. The sismotectonic context in Algeria is characterized mainly by reverse slip faults. Based on these definitions, the final Algerian database used to derive a prediction model covers 3–6.8 moment magnitude and 5–150 km hypocentral distance ranges respectively. Data has been processed with the Kinematics SWS (1989) and SMA (2001) softwares. Analog records were digitized using a 600 dpi scanner (Skarlatoudis et al. 2002) and processed with the Kinematics scanview software (1997). The sampling frequency for both digital and digitized analog data has been set to 200 sps. The Trifunac method (Trifunac et al. 1973) used for data processing is based on three steps: (1) instrument correction, (2) baseline correction of the acceleration data, and (3) high-pass filtering of velocity and displacement, using an Ormsby filter. For instrument correction the low-pass cut-off frequency of the Ormsby filter was set to 25 Hz for the SMA-1, SSA-1, and ETNA, with a 3 Hz roll-off width. The corner frequency for

both long-period baseline correction filtering and high-pass filtering of velocity and displacement, depends mainly on the spectral signal-to-noise ratio of each component, and has been estimated in the 0.12–0.2 Hz range with a roll-off width of 0.06 Hz and in the 0.2–0.3 Hz range with a roll-off width of 0.1 Hz for digital and analog data respectively. Douglas and Boore (2011) and Akkar et al. (2011) showed that PSA can often be used up to certain frequency higher than the high cut corner frequencies. According to Douglas and Boore (2011), this apparent contradiction can be explained by the fact that PSAs are often controlled by ground acceleration associated with much lower frequencies than the natural frequency of the oscillator. Also, according to Akkar et al. (2011), one can confidently use the spectral ordinates at periods beyond the low-cut corner period, for example, at a period that is just over half of the low-period filter cut-off. In our study, the PSA is computed for period ranging between 0.02 and 4.0 s.

However, since the distribution of Algerian data shows a lack of records for high magnitudes and in order to get an appropriate magnitude-distance distribution to ensure robust magnitude scaling one completed the database with 498 European strong motion records (Ambraseys et al. 2000) and 158 American records collected from USGS and the California Division of Mines and Geology (CDMG) strong motion databases with magnitude ranging between 5.2 to 7.0 and 5.8 to 7.4 respectively. As revealed by the performed analysis, the addition of regional data was necessary to predict reliable strong motion parameters for a given magnitude-distance scenario and site class. In total, 1391 horizontal components were selected with the assumption of the independence of the two horizontal components. These records come from 153 earthquakes (Table 1). Statistically, the data are for 52.84% of Algerian data, 35.80% of European data and 11.36% of American data. All the data are from shallow crustal earthquakes in active regions (e.g. western North America, Italy, Algeria, Greece, etc.) and has depths less than 30 km in such a way to agree with the Algerian seismotectonic context.

3 Truncation distance

As underlined by many authors (Joyner and Boore 1981; Boore et al. 1997, 2014; Fukushima and Tanaka 1990; Fukushima 1997; Fukushima et al. 2003), a selection criteria with respect to the magnitude and distance associated with each data must be used. Indeed, small events recorded far from the fault may disturb the data distribution and the regression results may be biased. In this study, one used two criteria; the first one truncates the far-distance data related to the type of recordings as shows in Fig. 3 (from Boore et al. 2014).

The second criterion truncates the far-distance data related to small events and predicted to be less than 10 cm/s^2 (Fukushima et al. 2003). To estimate the truncation distance, the Fukushima et al. (2000) GMPE's is used (Eq. 1).

$$\log 7 < 0.42 \cdot M - \log(R + 0.025 \cdot 10^{0.42M}) - 0.0033 \cdot R + 1.22 \quad (1)$$

where the logarithm is base 10.

Table 2 shows the distribution of data between Algeria, Europe and the USA before and after truncation process, as well as their relative percentage. One note that the truncation has mainly influenced the Algerian low magnitudes data because the Algerian database starts from the magnitude $M = 3.0$, whereas the other data start from the magnitude 5.2 for Europe and 5.8 for USA. The almost parity between the number of local and regional data

Table 1 List of earthquakes whose records are used in the regression analysis

No.	Earthquake name	Date	Time	Lat.	Lon.	Prof. (km)	M _w	No of records
<i>Algerian data</i>								
1	El-Asnam	21/10/80	16:50:51.6	36.31	1.72	10.00	4.5	04
2	El-Asnam	22/10/80	16:23:14	36.37	1.52	10.00	4.8	04
3	El-Asnam	23/10/80	9:57:55.1	36.42	1.53	10.00	4.6	02
4	El-Asnam	30/10/80	23:38:12.8	36.32	1.65	10.00	5.1	01
5	El-Asnam	08/11/80	7:54:18.2	36.11	1.36	10.00	5.3	01
6	Constantine	27/10/85	19:34:57.12	36.46	6.76	10.00	5.9	04
7	Chenoua	29/10/89	19:9:12.94	36.79	2.45	5.00	5.9	04
8	Mascara	18/08/94	1:13:5.78	35.52	– 0.11	8.00	5.9	08
9	AinBenian	04/09/96	4:14:3.21	36.98	2.88	10.00	5.5	08
10	BeniOurtilane	10/11/00	20:10:53.37	36.60	4.77	10.00	5.8	06
11	BeniOurtilane (AS)	16/11/00	11:33:9.3	36.66	4.76	10.00	4.9	06
12	BeniOurtilane (AS)	08/12/00	9:8:46.22	36.55	4.77	10.00	3.0	02
13	BeniOurtilane (AS)	11/12/00	17:52:10.53	36.46	4.78	10.00	4.4	02
14	Boumerdes	21/05/03	18:44:20.1	36.96	3.63	12.00	6.8	22
15	Boumerdes (AS)	21/05/03	18:51:10.3	36.97	3.81	10.00	5.7	02
16	Boumerdes (AS)	21/05/03	19:37:32.52	36.63	3.46	10.00	4.1	04
17	Boumerdes (AS)	21/05/03	20:52:39.89	36.62	3.61	10.00	3.6	04
18	Boumerdes (AS)	21/05/03	23:23:43.89	36.92	3.50	10.00	4.9	04
19	Boumerdes (AS)	25/05/03	0:5:35.94	36.84	3.49	10.00	3.9	02
20	Boumerdes (AS)	26/05/03	16:1:30.15	36.87	3.52	10.00	3.9	04
21	Boumerdes (AS)	27/05/03	17:11:28.82	36.94	3.58	8.00	5.8	06
22	Boumerdes (AS)	27/05/03	17:22:45.77	36.75	3.71	10.00	3.5	02
23	Boumerdes (AS)	27/05/03	17:33:25.9	36.92	3.64	10.00	3.6	02
24	Boumerdes (AS)	27/05/03	18:6:13.48	36.77	3.79	10.00	3.0	04

Table 1 continued

No.	Earthquake name	Date	Time	Lat.	Lon.	Prof. (km)	M _w	No of records
25	Boumerdes (AS)	27/05/03	22:11:21.49	36.72	3.72	10.00	3.2	04
26	Boumerdes (AS)	28/05/03	6:58:37.65	36.88	3.27	10.00	5.0	08
27	Boumerdes (AS)	28/05/03	11:26:26.9	36.97	3.59	10.00	3.5	04
28	Boumerdes (AS)	28/05/03	19:5:20.07	37.06	3.65	10.00	4.3	06
29	Boumerdes (AS)	29/05/03	1:54:50.62	36.85	3.68	10.00	3.4	06
30	Boumerdes (AS)	29/05/03	2:14:59.83	36.82	3.36	10.00	5.2	10
31	Boumerdes (AS)	29/05/03	2:21:53.8	36.70	3.36	10.00	3.2	10
32	Boumerdes (AS)	29/05/03	5:2:57.21	36.68	3.57	10.00	3.0	08
33	Boumerdes (AS)	29/05/03	19:43:14.99	36.67	3.83	10.00	3.6	06
34	Boumerdes (AS)	31/05/03	17:35:28.35	36.79	3.65	10.00	3.2	10
35	Boumerdes (AS)	01/06/03	9:0:47.81	36.63	3.68	10.00	3.2	06
36	Boumerdes (AS)	01/06/03	22:54:32.39	36.80	3.51	10.00	3.3	06
37	Boumerdes (AS)	02/06/03	8:20:18.63	36.82	3.47	10.00	3.6	08
38	Boumerdes (AS)	02/06/03	22:30:55.96	36.84	3.46	10.00	4.1	06
39	Boumerdes (AS)	04/06/03	8:10:50.19	36.59	3.48	10.00	3.7	06
40	Boumerdes (AS)	05/06/03	21:54:34.51	36.66	3.51	10.00	3.0	06
41	Boumerdes (AS)	23/06/03	10:35:4.37	37.13	3.84	10.00	3.9	10
42	Boumerdes (AS)	05/07/03	20:3:33.52	37.24	3.65	10.00	4.5	06
43	Boumerdes (AS)	06/07/03	2:56:4.76	36.87	3.90	10.00	3.9	06
44	Boumerdes (AS)	06/07/03	8:50:16.02	36.81	3.65	10.00	3.5	06
45	Boumerdes (AS)	07/07/03	1:22:43.71	36.77	3.50	10.00	3.0	04
46	Boumerdes (AS)	14/07/03	22:52:21.36	36.75	3.53	10.00	4.1	08
47	Boumerdes (AS)	17/07/03	21:7:44.4	36.52	3.54	10.00	3.6	08
48	Boumerdes (AS)	26/07/03	7:59:58.29	36.85	3.73	10.00	3.4	10
49	Boumerdes (AS)	03/08/03	9:56:40.79	36.54	3.62	10.00	3.2	10

Table 1 continued

No.	Earthquake name	Date	Time	Lat.	Lon.	Prof. (km)	M _w	No of records
50	Boumerdes (AS)	11/08/03	20:3:41.27	36.67	3.56	10.00	3.6	08
51	Boumerdes (AS)	03/09/03	14:4:43.86	36.92	3.88	10.00	3.8	12
52	Boumerdes (AS)	08/09/03	7:44:10.73	36.69	3.60	10.00	3.4	12
53	Boumerdes (AS)	16/09/03	5:16:31.64	36.68	3.80	10.00	3.4	12
54	Boumerdes (AS)	12/10/03	7:8:42.94	37.00	3.48	10.00	3.8	12
55	Boumerdes (AS)	16/10/03	6:38:4.4	36.45	3.63	10.00	3.6	16
56	Boumerdes (AS)	19/10/03	4:52:23.74	36.76	3.40	10.00	3.2	14
57	Boumerdes (AS)	11/11/03	17:47:36.63	36.74	3.54	10.00	3.2	12
58	Boumerdes	10/01/04	18:38:14.81	36.85	3.42	10.00	4.5	30
59	Boumerdes	02/02/04	15:30:38.46	36.86	3.62	10.00	3.5	16
60	Boumerdes	23/02/04	16:13:28.13	36.83	3.69	10.00	3.4	16
61	Boumerdes	16/06/04	17:29:11.53	36.74	3.32	10.00	3.8	12
62	Boumerdes	01/12/04	17:42:24.79	36.85	3.45	10.00	4.5	30
63	Boumerdes	05/12/04	8:30:59.59	36.87	3.42	10.00	4.5	30
64	Boumerdes	02/07/05	7:42:48.89	36.83	3.45	10.00	4.1	12
65	Laalam	20/03/06	19:44:25.19	36.62	5.33	10.00	5.0	10
66	Alger	22/07/06	13:22:22.5	36.72	3.11	10.00	3.7	16
67	Chlef	16/12/06	19:34:33.2	36.37	1.03	17.00	4.4	04
68	Oran	09/01/08	22:24:13	35.62	- 0.57	10.00	4.6	14
69	Boumerdes	01/02/08	7:3:3:40	36.83	3.47	10.00	4.6	24
70	Mila	02/06/08	17:37:47	36.27	6.15	10.00	4.5	06
71	Oran	06/06/08	20:2:57	35.88	- 0.66	10.00	5.5	24
72	Chlef	18/06/08	13:24:56	36.37	1.05	10	4.6	10
73	Mascara	21/12/09	02:45:12	32.98	0.25	10	4.3	06
74	Boumerdes	18/08/10	04:52:04	36.83	3.49	10	4.1	04

Table 1 continued

No.	Earthquake name	Date	Time	Lat.	Lon.	Prof. (km)	M _w	No of records
75	Douera	23/11/11	03:32:00	36.85	2.69	10	3.4	02
76	Chlef	04/03/12	02:45:00	36.37	1.04	10	4.6	20
77	Boumerdes	07/06/12	12:07:00	36.82	3.48	10	3.4	04
78	Bejaia	19/05/13	09:07:27	36.76	5.18	10	5.0	08
79	Ham Melouane 2013	17/07/13	03:00:00	36.24	2.80	10	4.8	06
80	Boumerdes 2014	22/02/14	19:30:34	36.82	3.64	10	4.3	10
81	Mostaganem 2014	22/08/14	00:22:46	35.72	0.16	10	4.0	10
82	Alger	01/08/14	04:11:16	36.856	3.181	10	5.5	32
<i>Regional data</i>								
83	Kern Country	21/07/52	04:53:00	35.00	119.03		7.2	8
84	Parkfield	27/06/66	20:26:00	35.90	120.90		6.2	9
85	Azores	28/02/69	02:40:31	35.97	10.58	14.00	7.6	2
86	San Fernando	09/02/71	06:01:00	34.40	118.40	8.00	6.6	8
87	Ionian	04/11/73	15:52:12	38.78	- 20.55	7.00	5.8	2
88	Azores	23/11/73	13:36:20	38.42	28.31	5.00	5.5	2
89	Friuli	06/05/76	20:00:13	46.32	- 13.32	6.00	6.5	20
90	Denizli	19/08/76	01:12:40	37.71	- 29.00	5.00	5.3	2
91	Friuli (AS)	11/09/76	16:31:10	46.30	- 13.23	6.00	5.7	12
92	Friuli (AS)	11/09/76	16:35:03	46.29	- 13.18	16.00	5.7	12
93	Friuli (AS)	15/09/76	09:21:19	46.32	- 13.16	12.00	6.1	28
94	Friuli (AS)	15/09/76	03:15:19	46.29	- 13.20	15.00	6.2	16
95	Caldiran	24/11/76	12:22:16	39.05	- 44.04	10.00	7.1	2
96	Ardal	06/04/77	13:36:37	31.90	- 50.76	10.00	6.1	1
97	Friuli	16/09/77	23:48:08	46.26	- 12.98	15.00	5.4	6
98	Ferruzano	11/03/78	19:20:48	38.02	- 16.03	15.00	5.3	4

Table 1 continued

No.	Earthquake name	Date	Time	Lat.	Lon.	Prof. (km)	M _w	No of records
99	Patti	15/04/78	23:33:48	38.27	- 14.86	15.00	5.9	8
100	Tabas	16/09/78	15:35:57	33.36	- 57.42	5.00	7.1	16
101	Montenegro (AS)	09/04/79	02:10:21	41.95	- 19.04	13.00	5.4	4
102	Montenegro (AS)	15/04/79	14:43:06	42.29	- 18.68	7.00	5.9	6
103	Montenegro	15/04/79	06:19:41	41.98	- 18.98	12.00	6.9	16
104	Montenegro (AS)	24/05/79	17:23:18	42.23	- 18.76	5.00	6.3	14
105	Coyote Lake	06/08/79	17:05:00	37.11	121.50	10.00	5.9	8
106	Valnerina	19/09/79	21:35:37	42.76	- 13.02	4.00	5.9	14
107	Imperial Valley	15/10/79	23:16:00	32.61	115.32	12.00	6.5	38
108	Azores	01/01/80	16:42:39	38.75	27.75	5.00	6.9	2
109	Campano Lucano	23/11/80	18:34:52	40.78	- 15.33	16.00	6.8	36
110	Campano Lucano (AS)	16/01/81	00:37:47	40.85	- 15.28	15.00	5.3	18
111	Alkion	24/02/81	20:53:37	38.10	- 22.84	10.00	6.6	2
112	Alkion	25/02/81	02:35:51	38.13	- 23.05	8.00	6.4	2
113	Preveza	10/03/81	15:16:20	39.20	- 20.80	10.00	5.5	4
114	Urmiya	23/07/81	00:05:33	37.11	- 45.21	20.00	5.8	2
115	Norcia	20/09/81	20:40:36	42.72	- 12.95	6.00	5.9	2
116	Ionian	17/01/83	12:41:30	38.07	- 20.25	14.00	6.9	2
117	Ionian	23/03/83	23:51:05	38.23	- 20.29	3.00	6.2	2
118	Biga	05/07/83	12:01:27	40.33	- 27.21	7.00	6.1	6
119	Kars	30/10/83	04:12:28	40.35	- 42.18	14.00	6.6	2
120	Umbria	29/04/84	05:02:59	43.25	- 12.47	7.00	5.6	12
121	Lazio Abruzzo	07/05/84	17:49:43	41.73	- 13.90	8.00	5.9	26
122	Lazio Abruzzo	11/05/84	10:41:50	41.77	- 13.91	8.00	5.5	14
123	Golbasi	05/05/86	03:35:38	38.02	- 37.79	4.00	6.0	2

Table 1 continued

No.	Earthquake name	Date	Time	Lat.	Lon.	Prof. (km)	M _w	No of records
124	Etolia	18/05/88	05:17:42	38.35	- 20.47	26.00	5.3	1
125	Killini	16/10/88	12:34:05	37.90	- 21.06	12.00	5.8	4
126	Spiatak (AS)	07/12/88	07:45:45	40.96	- 44.27	11.00	5.9	2
127	Spiatak	07/12/88	07:41:24	40.91	- 44.25	6.00	6.7	2
128	Loma Prieta	18/10/89	00:04:00	37.04	121.95	18.00	6.8	64
129	Chenoua	29/10/89	19:09:13	36.78	- 2.44	6.00	5.8	2
130	Purnari	16/06/90	02:16:18	39.27	- 20.55	29.00	5.5	2
131	Manjil	20/06/90	21:00:08	36.96	- 49.41	19.00	7.1	12
132	Manjil (AS)	21/08/90	03:47:31	37.09	- 49.59	8.00	5.3	2
133	Spiatak	16/12/90	15:45:51	41.37	- 43.72	28.00	5.3	18
134	Dzhava-Racha	29/04/91	09:12:48	42.39	- 43.68	6.00	6.8	p4
135	Dzhava-Racha (AS)	03/05/91	20:19:39	42.60	- 43.15	6.00	5.5	8
136	Dzhava-Racha (AS)	15/06/91	00:59:20	42.44	- 44.03	6.00	6.2	10
137	Erzincan	13/03/92	17:18:40	39.72	- 39.63	10.00	6.8	4
138	Pulumur	15/03/92	16:16:16	39.53	- 39.93	10.00	5.9	2
139	Petrolia	25/04/92	11:06:00	40.37	124.32	15.00	7.0	10
140	Landers	28/06/92	04:58:00	34.22	116.43	9.00	7.1	18
141	Izmir	06/11/92	19:08:09	38.16	- 27.00	17.00	6.1	2
142	Gulf of Corinth	18/11/92	21:19:41	38.26	- 22.37	15.00	5.8	2
143	Pyrgos	26/03/93	11:58:15	37.59	- 21.39	10.00	5.5	4
144	Mouzakatika	13/06/93	23:26:40	39.26	- 20.58	15.00	5.3	2
145	Patras	14/07/93	12:31:49	38.18	- 21.76	15.00	5.8	4
146	Gulf of Corinth	04/11/93	05:18:37	38.34	- 21.91	10.00	5.5	4
147	Strait of Gibraltar	23/12/93	14:22:34	36.80	2.98	18.00	5.3	2
148	Komilion	25/02/94	02:30:51	38.73	- 20.58	10.00	5.6	4

Table 1 continued

No.	Earthquake name	Date	Time	Lat.	Lon.	Prof. (km)	M _w	No of records
149	Umbro-Marchigiano	26/09/97	00:33:16	43.02	- 12.89	7.00	5.7	26
150	Umbro-Marchigiano	26/09/97	09:40:30	43.01	- 12.84	8.00	6.0	40
151	Umbro-Marchigiana (AS)	12/10/97	11:08:36	42.87	- 12.97	0.00	5.4	24
152	Umbro-Marchigiana (AS)	14/10/97	15:23:00	42.91	- 12.94	5.00	5.7	44
153	Umbro-Marchigiana (AS)	14/10/97	16:23:42	42.91	- 12.94	5.00	5.7	2

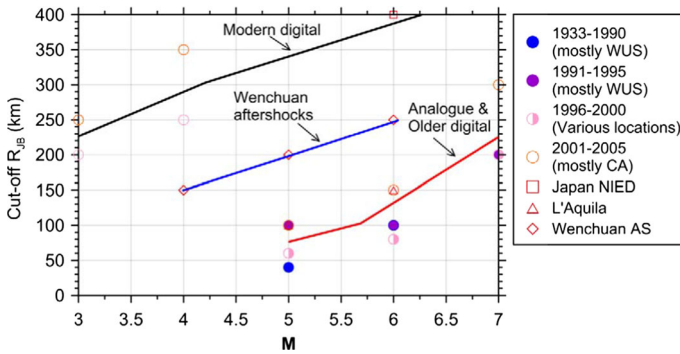


Fig. 3 Magnitude- and distance-dependent cutoff criteria for using records (Reproduced with permission from Boore et al. 2014)

Table 2 Record distribution between Algeria, Europe and the USA

	Before truncation		After truncation	
Algerian data	735	52.84%	556	46.03%
European data	498	35.80%	494	40.89%
USA data	158	11.36%	158	13.08%
Total	1391	100%	1208	100%

will allow both types of data to have a real impact on the prediction model and considering the Algerian seismotectonic context through the integration of sufficient data recorded in Algeria. Figure 4 shows the magnitude-distance distribution used to derive the spectral model prediction before and after the truncation distance. It remains 1208 records that are used to develop the ground motion predictive model for Algeria and neighboring regions whose distributions are 46.03, 40.89 and 13.06% for Algeria, Europe and the USA respectively. In order to test the impact of each category of data, two cases are study; the first one is based on local data, which will serve to illustrate the limits of considering the country’s borders only, and the second case consist of adding regional data in order to investigate their influence on the reliability and robustness of the developed model.

4 Site classification

In earthquake engineering, the practice consists to categorize sites into different general classes. Building codes have widely applied site classification schemes (such as surface geology, average shear wave velocity over 30 m (V_{s30}) etc.) to classify the sites into different categories (CEN 2004; RPA 2003, Building Seismic Safety Council (BSSC) 2000). The objective of site classification is to classify a group of strong-motion station sites into several classes so that the conditions within the same site class are similar (Rock, firm, soft, very soft). This makes it possible then to develop tools for engineers such design spectra and GMPEs taking into account the specificity of each site.

In the recent years, it has been shown that NHV for noise and EHV for seismic motions can supply useful information about the resonance properties of the shallow subsoil and

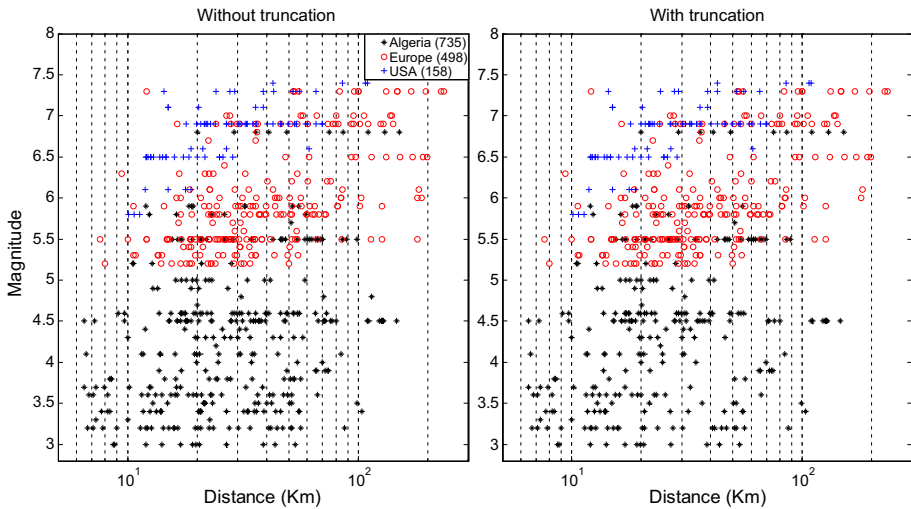


Fig. 4 Magnitude-distance distribution of data used to derive the spectral prediction model

represent a cost-effective tool for microzoning studies and site classifications and characterization of accelerometric networks which represent an important field of potential application of HVSR measurements. On the other hand, when the number of accelerometric sites is of the order of hundreds as for the case of the Algerian accelerograph network, the application of intensive seismic surveys (e.g. cross-hole or down-hole) requires funds beyond those commonly allocated on purpose. Presently, microtremor measurements providing direct information on the resonance soil frequencies allow the application of classification schemes alternative to those based on the single V_{s30} . In this way, several alternative classification schemes have been proposed (Zhao et al. 2006; Fukushima et al. 2007; Ghasemi et al. 2009; Di Alessandro et al. 2012; Beneldjouzi and Laouami 2015) that are based on the use of fundamental/predominant resonance frequency alone or in parallel to the V_{s30} .

Before this study, the Algerian data as well as the European and American data was originally classified as rock or soil based essentially on geological data. In the present study one adopts Zhao et al.’s method (2006). The site periods and corresponding frequencies to determine site classes are given in Table 3. As soil descriptions are not used in the present study, the four site classes are referred to as SC-I, SC-II, SC-III and SC-IV,

Table 3 Site natural period according to Zhao et al. (2006)

Site class	Site natural period (s) Zhao et al. (2006)	Average shear wave velocity (m/s)	Corresponding EC-8 soil classes	Corresponding RPA2003 soil classes
SC-I	$T_g < 0.20$ s	$V_{s30} > 600$	A	S1
SC-II	$0.20 \text{ s} \leq T_g < 0.40$ s	$300 < V_{s30} \leq 600$	B	S2
SC-III	$0.40 \text{ s} \leq T_g < 0.60$ s	$200 < V_{s30} \leq 300$	C	S3
SC-IV	$T_g \geq 0.60$ s	$V_{s30} \leq 200$	D	S4

instead of rock, hard soil, soft soil, and very soft soil sites, respectively corresponding to the following EC-8 (CEN 2004) soil classes A, B, C, and D and the Algerian soil classes (RPA 2003) S1, S2, S3 and S4 respectively (Table 3). In the present study, one uses the spectral ratio of horizontal and vertical components of earthquake records. Instead of Fourier spectral ratios, one proposes to use ratios of 5% damped response spectra which more advantageous than the Fourier spectra (Yamazaki and Ansary 1997; Zhao et al. 2006).

For each site, the H/V spectral ratio is computed following three steps: (1) select all the accelerometric recordings and calculate the pseudo response spectrum for the three components East–West, North–South and Vertical with a damping of 0.05 instead to use a smoothing function (Zhao et al. 2006), (2) calculate the ratios H/V from the response spectra North–South/Vertical, East–West/Vertical and the average of the two components, (3) calculate the geometrical mean and the standard deviation (σ) of the obtained spectral ratios.

The database consists of Algerian data and foreign data. For local data, the sites names and the record number per site are known. However, for foreign data, the station names are not available, and the records are known individually, so in this study, all sites were manually classified and an average H/V for each soil class is computed. In order to have robust statistics, even European and USA earthquakes with magnitude lower than 5.2 are used increasing the database to 1648 records. The average H/V is computed for each record having three components. Then, when information about the name of the station or site is available, the determination of the predominant period of each site was made after computing the average H/V spectral ratio over the events recorded at this site; then, an average curve and a standard deviation are associated with this site. This is the case for the Algerian data. For the other data, the two horizontal components are preceded as independent and the average H/V for each record is used. During the classification procedure, the observed H/V amplification and the related frequency band width are compared to the period intervals defined by Zhao et al. (2006) (Table 3). After achieving the classification of all the database, classification results are grouped into the four soil classes SC-I, SC-II, SC-III and SC-IV. The number of records in each soil class are shown in Table 4 and the magnitude-distance distributions of the four soil classes are plotted in Fig. 5 (top), while in Fig. 5 (bottom) are plotted the computed H/V spectral ratios, their means and \pm sigma. In the same figure, the site natural period intervals according to Zhao et al. (2006) are plotted with vertical dashed lines. Analysis of Table 4 underlines relatively very interesting samples from a statistical point of view. Indeed, except the soil class SC-IV which contains a small number of data, the other soil classes contain a fairly large and representative amount of data. Especially for the rock site class (SC-I) which is the basis for the development of the prediction model.

Figure 6 describes the comparison between the geometrical mean H/V spectral ratios and the associated standard deviations obtained for the 04 soil classes. The amplitudes and the shapes of the mean H/V spectral ratios are significantly different among the four soil

Table 4 Number of records in each soil class

Site class	No of records	EC-8	RPA99
SC-I	844	A	S1
SC-II	390	B	S2
SC-III	274	C	S3
SC-IV	140	D	S4

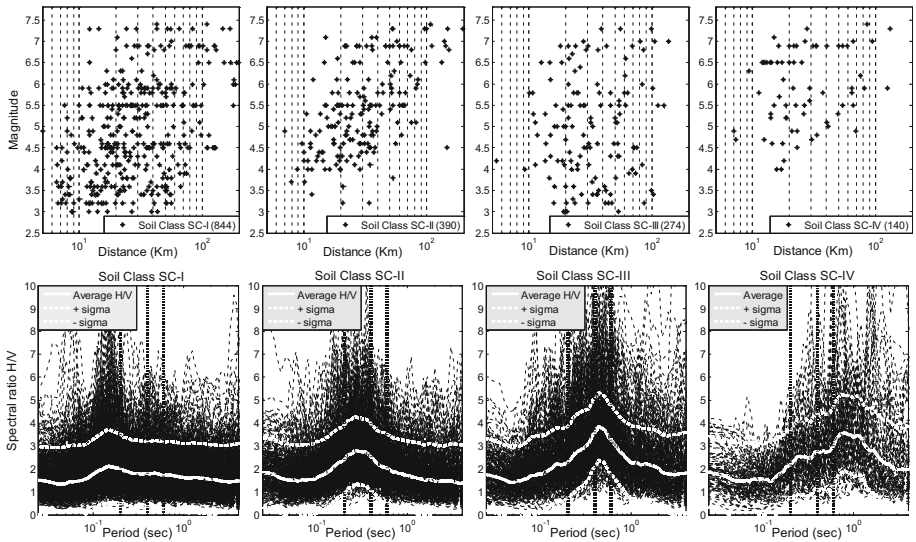


Fig. 5 Soil classes magnitude-distance distributions (top) and corresponding H/V spectral ratios, their means and \pm sigma (bottom). The site natural period intervals according to Zhao et al. (2006) are plotted with vertical dashed lines

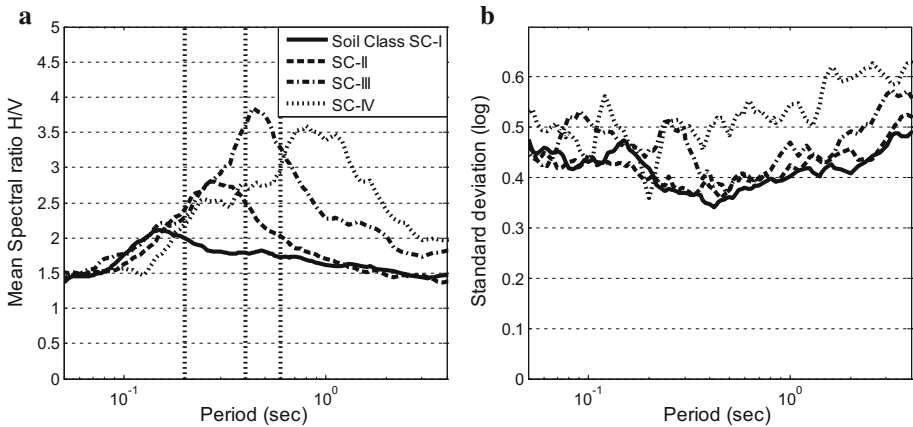


Fig. 6 Average H/V spectral ratios (a) and the associated standard deviations (b) obtained for the 04 soil classes. The site natural period intervals according to Zhao et al. (2006) are plotted with vertical dashed lines

classes. Figure 6a shows that the spectral ratios have peaks in the period range similar to those of site periods that have been defined for each site class by Zhao et al. (2006) (Table 3) and used in this study for the classification of the database. One can see that the average spectral ratios have peaks around 0.15, 0.26, 0.44, and 0.8 s for SC I, II, III and IV soil class respectively. This result demonstrates the accuracy of site classification performed on the basis of H/V spectral ratios.

In Fig. 6b, the standard deviation values in the natural logarithm scale have an average variation between 0.4 and 0.5. Indeed, the standard deviation and the peaks of the mean H/V ratios are respectively 0.51 at 0.15 s for SC I, 0.38 at 0.26 s for SC II, 0.39 at 0.44 s

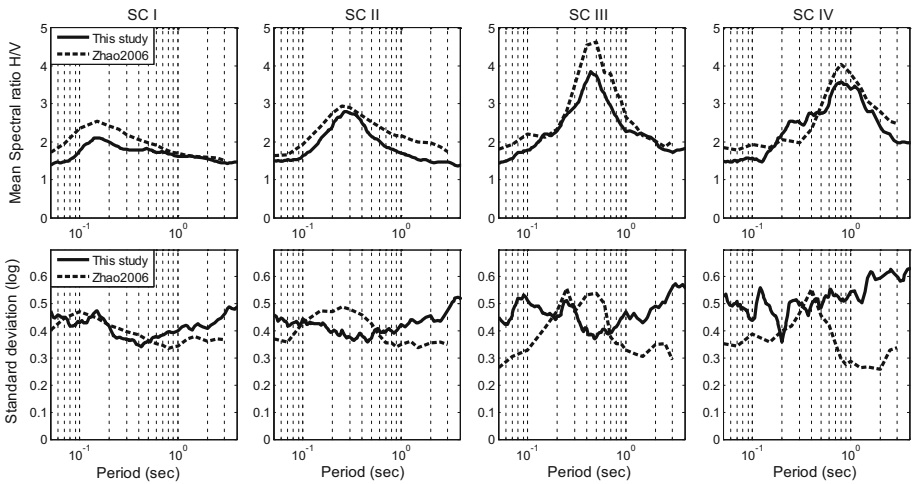


Fig. 7 Comparison between the computed mean H/V and the standard deviation for the 04 soil classes with the ones of Zhao et al. (2006)

for SC III and 0.51 at 0.8 s for SC IV. The largest standard deviation is for the soil class SC IV because of the relatively small value of the data (Table 4).

Figure 7 compares the computed mean H/V and the standard deviation for the 04 soil classes with the ones of Zhao et al. (2006). The mean spectral ratios show a good similarity between the present study and Zhao et al. (2006) results despite the fact that different data were used, namely Japanese and Euro-Mediterranean respectively. These results demonstrate that the classification has been successful. The standard deviations are comparable for soil classes SC I and SC II, and exhibit some differences for SC III and SC IV.

Moreover these results suggest that H/V spectral ratios can be used to assign site classes for developing ground motion prediction equations. The effect of the standard deviation, even if it is in the same order as obtained by other authors, may not be reliable in estimating site terms of GMPEs, considering the large variability of these predictive models.

Table 5 Mean H/V and associated standard deviations obtained by Zhao et al. (2006) for the Japanese data, Ghasemi et al. (2009) for Iranian data, Di Alessandro et al. (2012) for Italian data, and the present study

	Period (s)				Peak H/V				Sigma			
	SC I	SC II	SC III	SC IV	SC I	SC II	SC III	SC IV	SC I	SC II	SC III	SC IV
Zhao et al. (2006)	0.15	0.25	0.40	0.80	2.50	3.00	4.10	3.70	0.47	0.50	0.26	0.29
Ghasemi et al. (2009)	0.16	0.26	0.50		2.25	2.70	3.6		0.55	0.57	0.52	
Di Alessandro et al. (2012)	0.15	0.25	0.50	1.00	2.75	2.80	2.85	2.35	0.35	0.28	0.29	0.68
This study	0.15	0.26	0.44	0.80	2.10	2.80	3.85	3.58	0.47	0.38	0.39	0.51

Table 5 shows a comparison with the mean H/V and associated standard deviations obtained by Zhao et al. (2006) for the Japanese data, Ghasemi et al. (2009) for the Iranian data and Di Alessandro et al. (2012) for the Italian data. The comparison shows that the 04 studies give relatively similar periods for the 04 soil classes (only 03 for Ghasemi et al.), and small differences in regard to the H/V amplitudes at those periods. Otherwise, the standard deviation found in this study is in the same proportion with the one found by Zhao et al. (2006). For the Iranian data the standard deviation is more important, but for the Italian data, it has a high value for the SC IV site class.

It is evident that the relatively small value of the data for the soil class SC IV, suggests rejecting them from the GMPE. Therefore, one combines the SC III and SC IV soil classes into a single class SC-3 (SC III plus SC IV).

5 Spectral ground motion prediction equation

The ground motion prediction equation express earthquake ground motion parameters as function of simple parameters characterizing the earthquake source, the propagation path between the earthquake source and the site, and the geologic condition beneath the site. The general form of GMPE used in this study to predict the seismic motion in terms of response spectrum, accounts for geometrical spreading, anelastic attenuation and geological site condition. This model requires three parameters: magnitude, distance and site condition. The regression follows the two-step method (Fukushima and Tanaka 1990, 1992), introduced by Joyner and Boore (1981), which considers independently the magnitude and the distance. The GMPE describes the evolution of the spectral acceleration for 5% damping, $PSA(f)$, with respect to the magnitude, the hypocentral distance and the soil classes, following Eq. (2):

$$\log_{10} PSA(f) = a(f) \cdot M_w + b(f) \cdot d - \log_{10} d + c_{1,2,3}(f) + \sigma(f) \quad (2)$$

d being the hypocentral distance in km, and M_w the moment magnitude.

The anelastic attenuation coefficient $b(f)$ is determined in the first step, and in the second step, the magnitude coefficient $a(f)$ and the site effect coefficients $c_{1,2,3}(f)$ are computed. Coefficient c_1 is for rock sites (SC-I), c_2 for firm sites (SC-II) and c_3 for alluvium sites (SC-3). $\sigma(f)$ is the standard deviation, and f is the frequency in Hz. This equation form is similar to the one used by Berge-Thierry et al. (2003) and Liu and Tsai (2005). The model doesn't take into account the saturation effect, nor the hanging wall or the directivity effects, due to the absence of strong motion related with strong events in the near fault in the considered region and particularly in Algeria. Table 6 presents the period-dependent coefficients for median pseudo-spectral accelerations (5% damping for response spectra) and the associated standard deviations for some selected periods. The variation of the standard deviation σ versus the period shows a standard deviation of the PGA around 0.28. Both the truncation distance with respect to magnitude and distance and the site classification contributed to reducing the value of the standard deviation. For periods higher than 1 s, one found positive values for $b(f)$. However, according to the relationship between $Q(f)$ and the distance coefficient (Trifunac 1976), this correspond to a negative $Q(f)$. Spudich et al. (1997), Boore et al. (1997), Berge-Thierry et al. (2003) and Fukushima et al. (2003) have also observed a similar result. Therefore, in their study, Spudich et al. reset the negative Q value to zero. This assumption is adopted in this paper.

Table 6 Regression coefficients for median pseudo-spectral accelerations (5% damping for response spectra) and the associated standard deviations

T (s)	a	b	c ₁	c ₂	c ₃	σ
PGA	0.3872	− 0.0009	1.0240	1.0870	1.1390	0.2847
0.02	0.3796	− 0.0009	1.0820	1.1400	1.1930	0.2886
0.03	0.3551	− 0.0009	1.2700	1.3160	1.3570	0.2964
0.04	0.3370	− 0.0011	1.4540	1.4760	1.5200	0.3038
0.05	0.3281	− 0.0013	1.5740	1.5910	1.6320	0.3108
0.06	0.3275	− 0.0015	1.6240	1.6340	1.6670	0.3126
0.07	0.3370	− 0.0016	1.5990	1.6140	1.6410	0.3107
0.08	0.3390	− 0.0015	1.5980	1.6200	1.6540	0.3075
0.09	0.3442	− 0.0015	1.5850	1.6120	1.6460	0.3035
0.10	0.3494	− 0.0014	1.5650	1.5940	1.6260	0.3051
0.11	0.3593	− 0.0014	1.5230	1.5520	1.5840	0.3102
0.12	0.3726	− 0.0014	1.4560	1.4910	1.5100	0.3161
0.13	0.3857	− 0.0014	1.3810	1.4310	1.4380	0.3190
0.14	0.3958	− 0.0013	1.3160	1.3790	1.3800	0.3221
0.15	0.4083	− 0.0012	1.2280	1.3150	1.3030	0.3236
0.16	0.4236	− 0.0008	1.1190	1.2190	1.2020	0.3245
0.17	0.4375	− 0.0007	1.0250	1.1370	1.1160	0.3250
0.18	0.4513	− 0.0008	0.9311	1.0520	1.0380	0.3245
0.19	0.4620	− 0.0007	0.8489	0.9788	0.9736	0.3236
0.20	0.4714	− 0.0007	0.7725	0.9173	0.9139	0.3233
0.25	0.5048	− 0.0005	0.4849	0.6816	0.7009	0.3367
0.28	0.5303	− 0.0007	0.2897	0.4854	0.5295	0.3410
0.30	0.5460	− 0.0008	0.1773	0.3620	0.4166	0.3451
0.35	0.5843	− 0.0009	− 0.1081	0.0624	0.1420	0.3543
0.40	0.6077	− 0.0007	− 0.2898	− 0.1359	− 0.0186	0.3625
0.45	0.6311	− 0.0006	− 0.4857	− 0.3516	− 0.1996	0.3694
0.50	0.6512	− 0.0005	− 0.6473	− 0.5261	− 0.3591	0.3726
0.55	0.6712	− 0.0003	− 0.8268	− 0.7073	− 0.5457	0.3770
0.60	0.6832	− 0.0002	− 0.9384	− 0.8211	− 0.6542	0.3826
0.65	0.6977	− 0.0001	− 1.0510	− 0.9441	− 0.7661	0.3899
0.70	0.7192	− 0.0001	− 1.2140	− 1.1190	− 0.9355	0.3960
0.75	0.7316	− 0.0003	− 1.3240	− 1.2310	− 1.0560	0.3998
0.80	0.7428	− 0.0002	− 1.4260	− 1.3330	− 1.1660	0.4026
0.85	0.7550	− 0.0001	− 1.5370	− 1.4360	− 1.2800	0.4062
0.90	0.7650	0	− 1.6350	− 1.5280	− 1.3790	0.4072
1.00	0.7787	0	− 1.7900	− 1.6750	− 1.5310	0.4081
1.10	0.7910	− 0.0001	− 1.9240	− 1.8120	− 1.6600	0.4159
1.20	0.8057	− 0.0004	− 2.0520	− 1.9430	− 1.8030	0.4208
1.25	0.8123	− 0.0005	− 2.1130	− 2.0040	− 1.8690	0.4221
1.30	0.8177	− 0.0005	− 2.1710	− 2.0620	− 1.9340	0.4235
1.40	0.8276	− 0.0004	− 2.2800	− 2.1700	− 2.0560	0.4242
1.45	0.8301	− 0.0005	− 2.3070	− 2.1970	− 2.0850	0.4252
1.50	0.8355	− 0.0004	− 2.3730	− 2.2630	− 2.1560	0.4272

Table 6 continued

T (s)	a	b	c ₁	c ₂	c ₃	σ
1.60	0.8429	− 0.0004	− 2.4620	− 2.3520	− 2.2550	0.4289
1.65	0.8479	− 0.0005	− 2.5180	− 2.4140	− 2.3180	0.4292
1.80	0.8562	− 0.0006	− 2.6190	− 2.5220	− 2.4280	0.4325
2.00	0.8655	− 0.0010	− 2.7460	− 2.6520	− 2.5610	0.4386
2.20	0.8723	− 0.0010	− 2.8610	− 2.7600	− 2.6790	0.4392
2.40	0.8803	− 0.0011	− 2.9740	− 2.8610	− 2.7920	0.4393
2.50	0.8842	− 0.0011	− 3.0270	− 2.9130	− 2.8440	0.4396
2.60	0.8878	− 0.0012	− 3.0770	− 2.9630	− 2.8950	0.4408
2.80	0.8944	− 0.0011	− 3.1740	− 3.0580	− 2.9960	0.4463
3.00	0.9006	− 0.0011	− 3.2620	− 3.1480	− 3.0910	0.4503
3.20	0.9031	− 0.0012	− 3.3300	− 3.2170	− 3.1580	0.4538
3.30	0.9046	− 0.0012	− 3.3690	− 3.2570	− 3.1980	0.4549
3.40	0.9048	− 0.0013	− 3.3880	− 3.2740	− 3.2160	0.4552
3.60	0.9044	− 0.0014	− 3.4350	− 3.3170	− 3.2630	0.4562
3.80	0.9021	− 0.0015	− 3.4760	− 3.3530	− 3.3050	0.4562
4.00	0.8991	− 0.0015	− 3.5130	− 3.3870	− 3.3400	0.4536

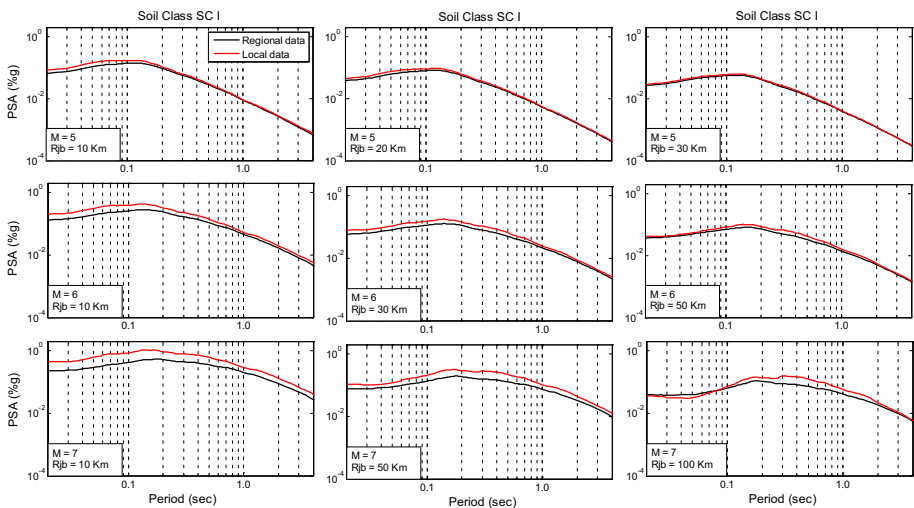


Fig. 8 PSA versus period for local and regional models

6 Prediction results and discussions

6.1 Local versus regional data

An analysis is made to examine the contribution of regional data to local data on the stability of the ground motion prediction equation. Two cases were studied. The first considers only local data with a maximum magnitude of 6.8, and the second incorporates European and few American data that contain magnitudes up to 7.4. In Fig. 8, the two

cases are compared for the rock soil class SC-I. and for magnitudes M5, M6 and M7. The variation of the PSA with period shows similar results for M5 and for $R_{jb} = 10, 20, 30$ km, slightly different for M6 and for $R_{jb} = 10, 30, 50$ km, but for large magnitude (M7) and for $R_{jb} = 10, 50, 100$ km, the local model overestimates the PSA.

In order to support the argument that not including the regional data in the database leads to overestimated ground motions, one compute the residuals between the actual data with the empirical predictions for both databases. Figures 9, 10 show graphs of the residuals values, the difference between the observed and the predicted values, for local and regional models, as function of magnitude (Fig. 9) and distance (Fig. 10) for PGA and spectral acceleration for 0.5, 1.0, and 5.0 Hz natural frequency together with linear best-fit

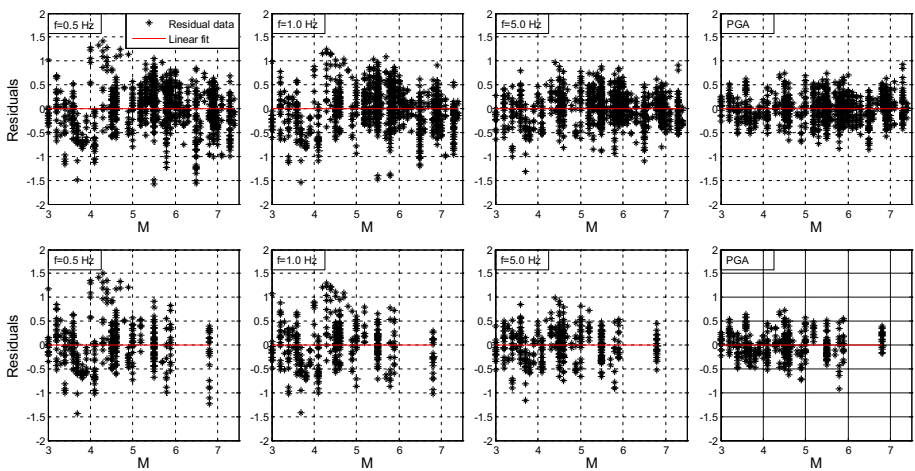


Fig. 9 Residuals against Magnitude for regional model (top) and local model (bottom) at 0.5, 1.0, 5.0 Hz and PGA

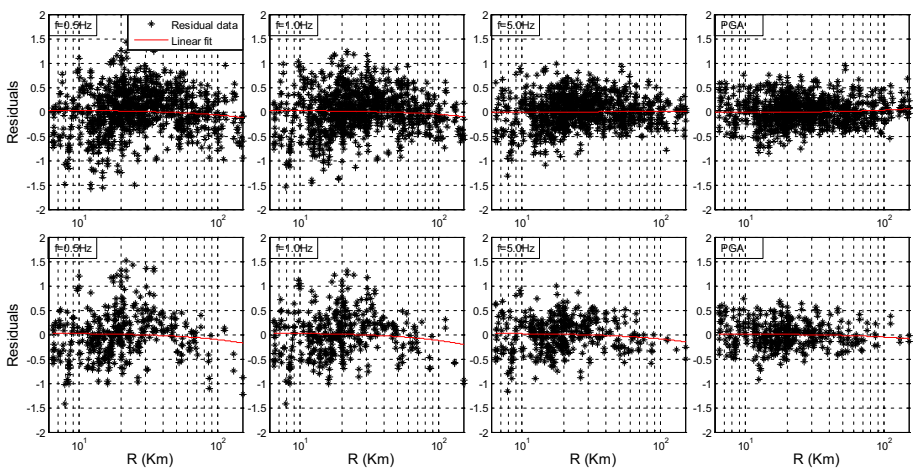


Fig. 10 Residuals against distance for regional data (top) and local data (bottom) at 0.5, 1.0, 5.0 Hz and PGA

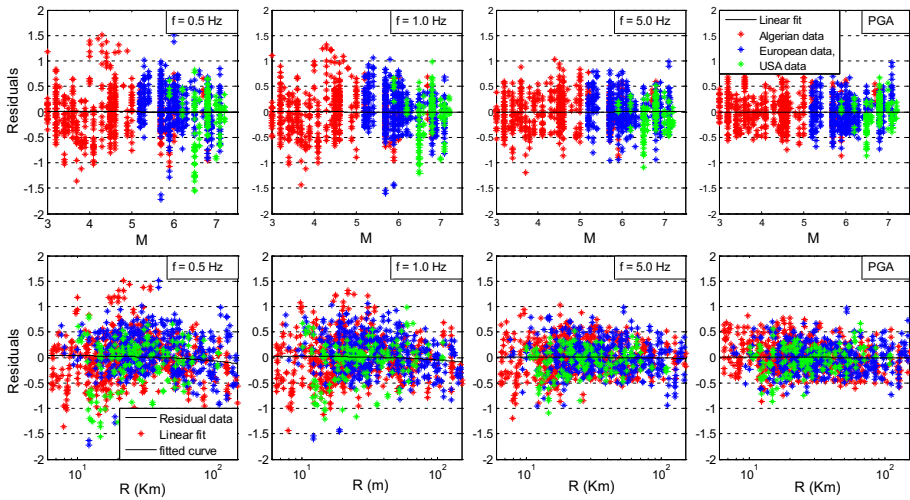


Fig. 11 Residuals versus origin data against magnitude (top) and distance (bottom) at 0.5, 1.0, 5.0 Hz and PGA

relations. With respect to magnitude no significant trends are observed for the full dataset. For distance, apparent linear trends are found particularly at large distance (> 100 km) at 0.5 Hz natural frequency in the case of regional data, while for local data, evident linear trends are evidenced for 0.5, 1.0, 5.0 Hz and PGA demonstrating the overestimation of the prediction model based on local data, as can be expected. This result confirms the importance of considering regional data and the limitations of considering only local data.

As one of the key aspects of the analysis was the inclusion of regional data in the final database, one plot in Fig. 11 the residuals values, for Algerian, European and American data, as function of Magnitude and distance for PGA and spectral acceleration for 0.5, 1.0, and 5.0 Hz natural frequency together with linear best-fit relations. With respect to the magnitude, no significant trends are observed for the data categories (local, EU, USA). For the distance, linear trends are found particularly at large distance (> 100 km) for 0.5 Hz natural frequency. This trend does not appear to be related to the origin of the data. This is due to the reduced amount of data in this distance range. All the residuals plots show no obvious dependence of the scatter on magnitude or distance. Despite the presence of some relative scarcity of data at low frequencies ($f = 0.5\text{--}1.0$ Hz), this apparent constant bias is common to all graphs of residuals for long period motions as related by Ambraseys et al. (2005). For the PGA, the residual values do not exhibit any systematic bias associated to a specific magnitude or distance.

6.2 Dependent period site coefficients

In order to estimate dependent period site coefficients for each soil classes, relative amplification are computed with respect to a reference class, which was assumed to be the SC-I soil class as follows:

$$Sc_{II}(T) = \frac{PSA^{SC-II}(T)}{PSA^{SC-I}(T)} \text{ for soil class SC-II and } Sc_{3}(T) = \frac{PSA^{SC-III}(T)}{PSA^{SC-I}(T)} \text{ for soil class SC-3.}$$

Figure 12 shows the predicted site coefficients for soil classes SC-II (a) and SC-3 (b) compared with the associated mean spectral ratio H/V, and the ratio between the mean

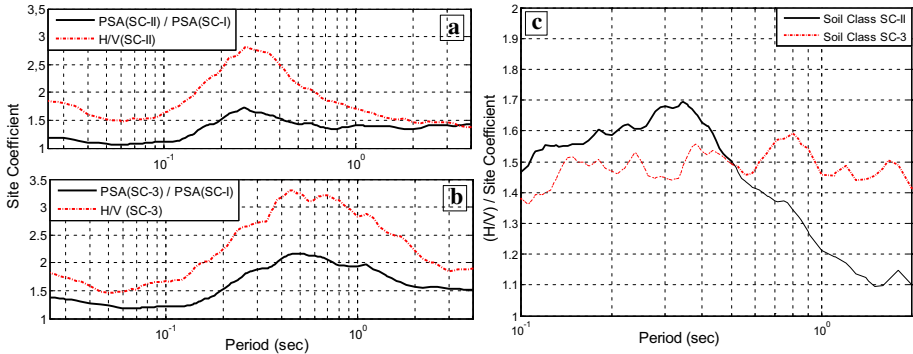


Fig. 12 Predicted period dependent site coefficients and the spectral ratio H/V for soil classes **a** SC-II and **b** SC-3, and the ratio between the mean spectral ratio (H/V) and the estimated period dependent site coefficient (**c**)

spectral ratio (H/V) and the site coefficient (**c**). From the plotted curves, the following remarks can be done:

1. The predicted site coefficient have peaks in the period range similar to those of site periods that have been defined for each site class by Zhao et al. (2006) (Table 3) and used in this study for the classification of the database. One can see that the SC-II and SC-3 show the maximum site coefficients of about 1.73 and 2.17 around 0.26 and 0.5 s respectively. As indicated in Fig. 12a, b the site coefficients related to the PGA ($T = 0$) are 1.22 and 1.43 for SC-II and SC-3 respectively. These values are in agreement with the EC-8 soil parameters given in Table 7. As the obtained soil coefficients were computed from the complete database, they are magnitude and distance independent. However, the EC-8 soil parameters are magnitude dependent and given for type 1 ($M > 5.5$) and for type 2 ($M < 5.5$). For comparison purpose, one considers a mean value for each soil class. It appears that soil coefficients for soil class SC-II (this study), soil class B (EC-8), SC-3 (which is the combination of SC III and SC IV soil classes in this study) and soil class CD (C plus D in EC-8) are very similar.
2. The period dependent site coefficients appear to be close to the mean spectral ratio H/V both in terms of spectral shape and peaks periods. This implies a good agreement between the site classification and the model prediction.

Figure 12c shows ratios between the mean spectral ratio H/V and the period dependent site coefficient computed for the soil classes SC-II and SC-3. For each soil class, the ratio is plotted in bold for the period interval according to the Zhao’s site classification adopted in this study. The intersection point between the two curves is in fact the period transition between the soil classes SC-II and SC-3. It appears that these ratios are around 1.5 for both

Table 7 Comparison between soil coefficient for PGA from EC-8 and this study

Soil class	EC-8			This study	
	B	C	D	SC-II	SC-3
Type 1	1.20	1.15	1.35		
Type 2	1.35	1.50	1.80		
Mean	1.27	1.44		1.22	1.43

the SC-II and SC-3 soil classes in their period intervals. Based on theoretical approach, Kawase et al. (2011) developed relationship between the spectral ratio H/V and the transfer function of a soil profile as follows: $\frac{H(\omega)}{V(\omega)} = \sqrt{\frac{V_p}{V_s} \frac{|TF_1(\omega)|}{|TF_3(\omega)|}}$ where $TF_1(\omega)$ is a transfer function for the horizontal motion due to the S wave, and $TF_2(\omega)$ is a transfer function for the vertical motion due to the P wave, V_p and V_s are respectively the P and S wave velocities. One can notice the similarity between the value of the ratio equal to 1.5 found in this study and the ratio $\sqrt{V_p/V_s}$ which has a mean value around 1.4 and 1.6 respectively for soil class SC-II and SC-3. In this comparison, one do not expect to find an analogy between the two approaches, but only to explain the ratio found between the H/V spectral ratio and the period dependent site coefficient.

6.3 Comparison to previous equations

The estimated ground motions from the equations derived in this study were compared with some recent well-known GMPEs developed in the same sismotectonic context i.e. shallow crustal earthquakes and active regions. The median estimations are compared to Ambraseys et al. (2005), Boore and Atkinson (2008), Akkar et al. (2010, 2013) and Boore et al. (2014). Three magnitude levels (M5, M6 and M7) are used in the comparisons that can encompass small, moderate and strong earthquakes in Algeria and surrounding regions. As indicated beforehand, the developed ground motion prediction equation considers the hypocentral distance. However, the most recent models incorporate the Joyner and Boore or the rupture distance. Also, for an appropriate use of the proposed model one performs conversion between the hypocentral distance R_{hyp} and the ‘Joyner-Boore’ distance R_{jb} (Sabetta et al. 2005). Based on the work of Sabetta et al. (2005; Table 7) one derive the following empirical relationships for small, moderate and large magnitudes (Fig. 13).

Figure 14 shows the predicted peak ground acceleration (PSA at $T = 0$ s) and spectral acceleration at 1.0 s natural period with distance for $M = 5, 6$ and 7 reverse faulting earthquakes at a rock site. For small earthquake ($M = 5.0$), one observes a large variability between the models which could be due to the lower magnitude bounds considered by the different GMPE’s. In this study, the lower magnitude limit is M3, the same value as Boore et al. (2014), while those used by Ambraseys et al. (2005), Boore and Atkinson (2008), Akkar et al. (2010, 2013) are between M4 and M5. This aspect was underlined recently by

$$\begin{aligned}
 &M \leq 5.5 \\
 R_{jb} &= \begin{cases} (R_{hyp} - 6.78)/0.625 & \text{for } (R_{hyp} < 10) \\ (R_{hyp} - 4.92)/0.974 & \text{for } (R_{hyp} \geq 10) \end{cases} \\
 &5.5 < M \leq 6.5 \\
 R_{jb} &= \begin{cases} (R_{hyp} - 9.15)/0.65 & \text{for } (R_{hyp} < 12.4) \\ (R_{hyp} - 7.45)/0.98 & \text{for } (R_{hyp} \geq 12.4) \end{cases} \\
 &6.5 < M \leq 7.5 \\
 R_{jb} &= \begin{cases} (R_{hyp} - 13.93)/0.775 & \text{for } (R_{hyp} < 18) \\ (R_{hyp} - 13.06)/1.02 & \text{for } (R_{hyp} \geq 18) \end{cases}
 \end{aligned}$$

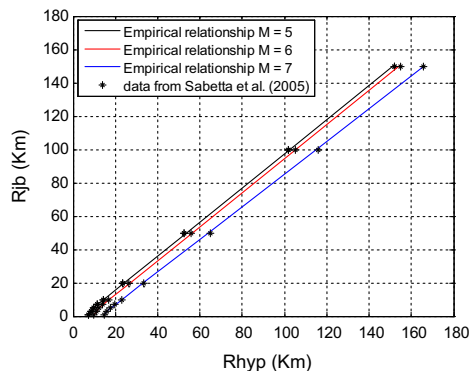


Fig. 13 Distance conversion between R_{jb} and R_{hyp}

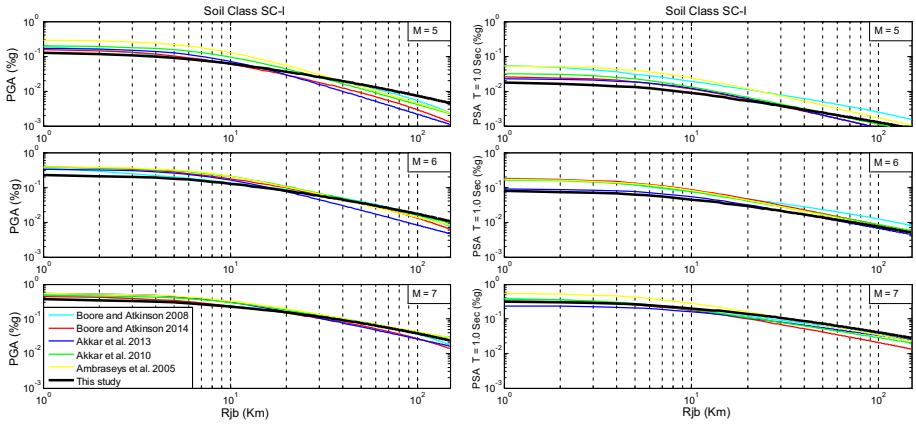


Fig. 14 Predicted peak ground acceleration and spectral acceleration at 1.0 s natural period with distance for M = 5, 6 and 7 reverse faulting earthquakes at a rock site and comparison with published models

Akkar et al. (2013) and Boore et al. (2014) who pointed out that the predicted accelerations are overestimated for largest lower magnitude limit.

The comparison with the published models in term of PGA and spectral acceleration for 1.0 s natural frequency reveals different trends. At short distance, the proposed GMPE for Algeria predicts relatively smaller peak ground acceleration up to 10, 20 and 30 km for magnitude M5, M6 and M7 respectively. For large distances and especially for M5, the model seems to overestimate the PGA. This result can be explained by the M-R distribution (Fig. 4) which reveals a lack of data for distances greater than 40 km associated with magnitude M5. Globally, the proposed model is closer to the models of Boore et al. (2014) and Akkar et al. (2013).

Figure 15 shows the predicted peak spectral acceleration versus period for M = 5, 6 and 7 reverse faulting earthquakes at rock (SC-I) site. In order to consider the accelerations which have an effect and comparable to the minimum required by the seismic engineering

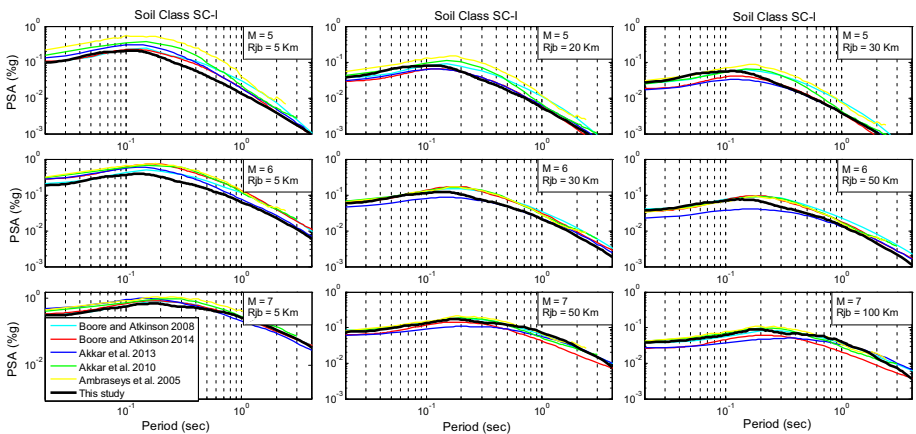
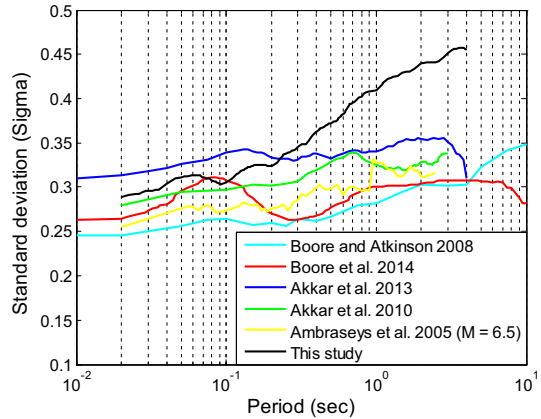


Fig. 15 Predicted peak spectral acceleration with period for M = 5, 6 and 7 reverse faulting earthquakes at a rock site and comparison with published models

Fig. 16 Standard deviation as function of period

codes, comparison with Ambraseys et al. (2005), Boore and Atkinson (2008), Akkar et al. (2010, 2013) and Boore et al. (2014) are performed for $R_{jb} = 5, 20, 30$ km and $M = 5.0$, for $R_{jb} = 5, 30, 50$ km and $M = 6.0$, and for $R_{jb} = 5, 50, 100$ km and $M = 7.0$. For example, for $(M, R_{jb}) = [(5.0, 30), (6.0, 50), (7.0, 100)]$ the predicted average acceleration is around 0.03 g which is lower than the lower acceleration required by the Algerian seismic code (0.07 g). For small distances ($R = 5$ km), the model predicts spectral accelerations slightly lower than the other models, but closer to the models of Akkar et al. (2013) and Boore et al. (2014), for the three considered magnitudes. For the intermediate and large distances, and for the magnitudes $M5$ and $M6$, a good similarity is observed with the models of Akkar et al. (2013) and Boore et al. (2014) for periods beyond 0.2 s. However, for the magnitude $M7$, the model predicts spectral accelerations closer to the models of Akkar et al. (2010) and Ambraseys et al. (2005). Figure 16 shows the period-dependent variation of the total standard deviation for the GMPEs derived in this study and compared to those of Ambraseys et al. (2005), Boore and Atkinson (2008), Akkar et al. (2010, 2013) and Boore et al. (2014). In the period range up to 0.23 s, one observes a good similarity between the models. Beyond, our sigma increases with the period, probably due to the amount of small M data. The Boore and Atkinson (2008) model constitutes the lower bound of the six set of GMPEs.

The quantification of site effects was clearly demonstrated by the computation of period dependent site coefficients for soil classes SC-II and SC-3 (Fig. 12). Their effects were then analyzed on the predicted spectral accelerations and compared to the published models. The comparison is appropriate with Akkar et al. (2010) and Ambraseys et al. (2005) models because they use the same definition of the site effect based on soil class. However, for Boore and Atkinson (2008), Akkar et al. (2013) and Boore et al. (2014), the site effect is introduced via the time averaged shear wave velocity at 30 m, V_{s30} , and is therefore site specific.

Figure 17 shows the comparison of estimated ratio of horizontal response spectral acceleration for ground motions on soft soil sites (SC-3) and rock sites (SC-I) (Fig. 17a) and on stiff soil sites (SC-II) and rock sites (SC-I) (Fig. 17b), derived in this study, with those of Ambraseys et al. (2005) and Akkar et al. (2010) as those two models used the same definition of site effect related to soil class, while the models of Akkar et al. (2013) and Boore et al. (2014) use site-specific shear wave velocity V_{s30} . The maximum of the site coefficient is reached for soft soil (SC-3) at 0.5 s for the proposed model, and at 1.3 and

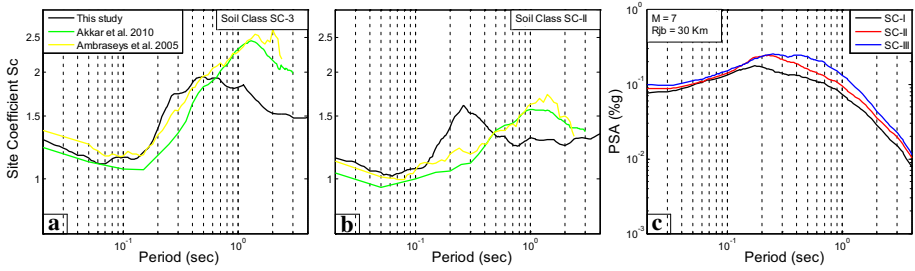


Fig. 17 Comparison of estimated ratio of horizontal response spectral acceleration for ground motions on **a** soft soil sites (SC-3) and rock sites (SC-I) and on **b** stiff soil sites (SC-II) and rock sites (SC-I), derived in this study with some previous studies (Akkar et al. 2010; Ambraseys et al. 2005), and **c** predicted peak spectral acceleration predicted on SC-I, SC-II and SC-3

1.5 s for Akkar et al. (2010) and Ambraseys et al. (2005) models respectively, and for firm soil (SC-II), it is reached at 0.26 s for the proposed model and at 1.0 and 1.2 s for Akkar et al. (2010) and Ambraseys et al. (2005) models respectively. This comparison reveals that the site effect predicted by the proposed model agrees with the soil classification defined for each site class by Zhao et al. (2006) (Table 3) and used in this study for the classification of the database. However, the site effect predicted by Ambraseys et al. (2005) and Akkar et al. (2010) do not allow distinguishing between the firm (SC-II) and soft (SC-3) soil classes with regard to the frequency content. It can also be pointed out that the site coefficient derived from our model is higher than those given by the two other models, for periods ranging between 0.1 and 0.5 s for both SC3 and SCII. One investigates the implication of the site effect coefficients on the predicted spectral acceleration. Figure 17c compares the peak spectral acceleration versus period obtained for soil classes SC-I, SC-II and SC-3. The results for site response effects look perfectly reasonable.

How the proposed model takes into account site effects for soil classes SC-II and SC-3 is shown in Figs. 18 and 19 through a comparison with the models of Ambraseys et al. (2005) and Akkar et al. (2010). The comparison is made for the same magnitudes and distances as in the case of the rocky site. For small, moderate and strong earthquake

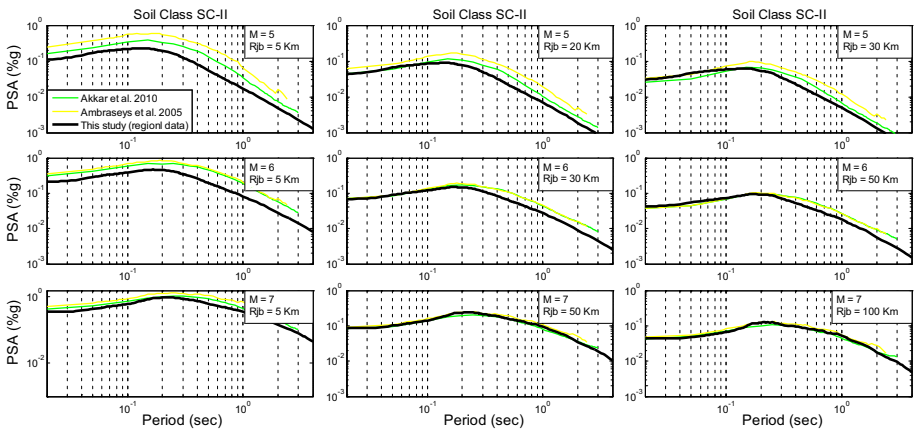


Fig. 18 Predicted peak spectral acceleration with period for M = 5, 6 and 7 reverse faulting earthquakes at a firm site and comparison with published models

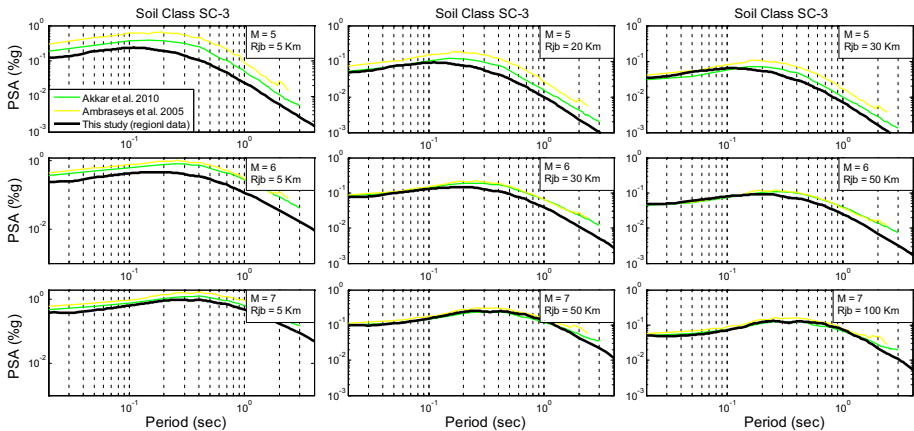


Fig. 19 Predicted peak spectral acceleration with period for $M = 5, 6$ and 7 reverse faulting earthquakes at a soft site and comparison with published models

($M = 5, 6$ and 7) at near distance ($R_{jb} = 5$ km), and for soil classes SC-II and SC-3, the predictions of the proposed model are below the equations of Akkar et al. (2010) and Ambraseys et al. (2005). This is the same trend as in the case of the soil class SC-I.

For small and moderate earthquake ($M = 5, 6$), and for intermediate ($R_{jb} = 20, 30$) and far distance ($R_{jb} = 30, 50$), our predictions for soil class SC-II are globally similar to those of Akkar et al. (2010) for period up to 0.2 s and below after. However, for strong earthquake ($M = 7$), at $R_{jb} = 50$ and 100 km, our predictions are similar to both Ambraseys et al. (2005) and Akkar et al. (2010). For soil class SC-3, a good similarity can be noticed with the model of Akkar et al. (2010). One would have liked to extend this comparison to the other models considered in this study. Unfortunately, because of their definitions of site effects based V_{s30} , different from ours which is based on coefficients related to soil classes, the comparison would have been biased.

It seems through this comparison that the model developed from a database that contains more than 50% of local records predicts slightly lower peak ground accelerations than the other models in near distances. Moreover, in the context of the assessment of the regional seismic hazard in Algeria, these results show that the models that can be used in the Algerian seismotectonic context are those of Boore et al. (2014) and Akkar et al. (2013), while the Ambraseys et al. (2005) and Akkar et al. (2010) GMPEs seem to overestimate the spectral accelerations.

7 Conclusion

In the framework of Algeria's seismic hazard assessment, a new spectral ground motion prediction equation is derived, using 1391 strong motions database, which contains more than 700 data recorded in Algeria completed with a similar number of Mediterranean region data and few American data. In this study, one used a site classification approach based on the predominant period computed from average H/V spectral ratio. Three soil classes for the calculation of the empirical spectral ground motion prediction relations are considered: rock, firm and soft. From the obtained results, one can make the following conclusions:

1. Statistically, the database used in this study is constituted by 52.84% of Algerian data, 35.80% of European data and 11.36% of American data. All the data are from shallow crustal earthquakes in active regions with depths less than 30 km to agree with the Algerian seismotectonic context.
2. A selection criteria with respect to the magnitude and distance associated with each data was used. This operation allows to prevent small events recorded far from the fault may disturb the data distribution and the regression results may be biased.
3. Classification site results, grouped into the four (04) soil classes SC-I, SC-II, SC-III and SC-IV, underline very interesting samples from a statistical point of view: 844, 390, 274 and 140 data for SC-I, SC-II, SC-III and SC-IV respectively.
4. The amplitudes and the shapes of the mean H/V spectral ratios are remarkably different among the four soil classes. The spectral ratios have peaks in the period range remarkably similar to those of site periods that have been defined for each site class by Zhao et al. (2006) and used in this study for the classification of the database.
5. A comparison with the mean H/V and associated standard deviations obtained by Zhao et al. (2006) for the Japanese data, Ghasemi et al. (2009) for Iranian data and Di Alessandro et al. (2012) for Italian data shows that the 04 studies give relatively similar periods for the 04 soil classes, and small differences with regard to the H/V amplitudes at those periods. Otherwise, the standard deviation found in this study is in the same proportion with the one found by Zhao et al. (2006).
6. The analysis of the effect of the local versus regional data on the reliability of the derived ground motion prediction equation shows the importance of completing the local database by regional records instead of being limited to local records only, which can give misleading results.
7. Dependent period soil coefficients which are the relative amplification with respect to the rock soil class are derived for SC-II and the SC-3 soil classes. The obtained results appear to be close to the mean spectral ratio H/V in terms of spectral shape and peaks periods. This implies a good agreement between the site classification and the model prediction, and underlines a direct relationship between the H/V spectral ratio and the period dependent site coefficient.
8. Comparisons with the GMPEs of Ambraseys et al. (2005), Boore and Atkinson (2008), Akkar et al. (2010, 2013) and Boore et al. (2014) show that the proposed model predicts slightly lower accelerations than the other models in short distances. Otherwise, it predicts spectral accelerations close to Akkar et al. (2013) and Boore et al. (2014). Consequently, Boore et al. (2014) and Akkar et al. (2013) GMPEs seem to be the most appropriate, with the developed model, for a better quantification of the seismic hazard in Algeria.
9. Finally, residual analysis with respect to magnitude shows no significant trends for the full dataset. For distance, apparent linear trends are found particularly at large distance (> 100 km) for 0.5 Hz natural frequency.

Acknowledgements The authors thank CGS accelerograph network operators and the technical staff for rigorously maintaining the Algerian Accelerograph Network. We are thankful to Fabrice Cotton for his help and for providing us with the accelerometric data from Europe and USA. We also thank the associate editor John Douglas and the anonymous reviewers for their constructive criticism and precious suggestions that helped us to improve this study.

References

- Abrahamson N, Silva W (2008) Summary of the Abrahamson and Silva NGA ground-motion relations. *Earthq Spectra* 24:67–97. <https://doi.org/10.1193/1.2924360>
- Akkar S, Bommer JJ (2010) Empirical equations for the prediction of PGA, PGV and spectral accelerations in Europe, the Mediterranean region and the Middle East. *Seismol Res Lett* 81:195–206
- Akkar S, Cagnan Z, Yenier E, Erdogan O, Sandikkaya MA, Gulkan P (2010) The recently compiled Turkish strong motion database: preliminary investigation for seismological parameters. *J Seismol*. <https://doi.org/10.1007/s10950-009-9176-9>
- Akkar S, Kale O, Yenier E, Bommer JJ (2011) The high-frequency limit of usable response spectral ordinates from filtered analogue and digital strong-motion accelerograms. *Earthq Eng Struct Dyn* 40:1387–1401. <https://doi.org/10.1002/eqe.1095>
- Akkar S, Sandikkaya MA, Bommer JJ (2013) Empirical ground-motion models for point- and extended-source crustal earthquake scenarios in Europe and the Middle East. *Bull Earthq Eng*. <https://doi.org/10.1007/s10518-013-9461-4>
- Ambraseys N, Smit P, Berardi R, Rinaldis D, Cotton F, Berge C (2000) Dissemination of European strong motion data. CD-ROM collection. European Commission, Directorate XII, Environmental and Climate Programme, ENV4-CT97-0397, Brussel, Belgium
- Ambraseys NN, Douglas J, Sarma SK, Smit PM (2005) Equations for the estimation of strong ground motions from shallow crustal earthquakes using data from Europe and the Middle East: horizontal peak ground acceleration and spectral acceleration. *Bull Earthq Eng* 3:1–53. <https://doi.org/10.1007/s10518-005-0183-0>
- Atkinson GM, Boore DM (2011) Modifications to existing ground-motion prediction equations in light of new data. *Bull Seismol Soc Am* 101:1121–1135
- Beneldjouzi M, Laouami N (2015) A stochastic based approach for a new site classification method: application to the Algerian seismic code. *Earthq Eng Eng Vib* 14:663–681
- Berge-Thierry C, Cotton F, Scotti O, Pommer DA, Fukushima Y (2003) New empirical response spectral attenuation laws for moderate European earthquakes. *J Earthq Eng* 7:193–222
- Boore DM, Atkinson GM (2008) Ground-motion prediction equations for the average horizontal component of PGA, PGV, and 5%-damped PSA at spectral periods between 0.01 and 10.0s. *Earthq Spectra* 24:99–138
- Boore DM, Joyner WB, Fumal TE (1997) Equation for estimating horizontal response spectra and peak acceleration from western North American earthquakes: a summary of recent work. *Seismol Res Lett* 68:128–153
- Boore DM, Stewart JP, Seyhan E, Atkinson GM (2014) NGA-West2 equations for predicting PGA, PGV, and 5%-damped PSA for shallow crustal earthquakes. *Earthq Spectra* 30:1057–1085
- Bracene R, Patriat M, Ellouz N, Gaulier JM (2003) Subsidence history in basins of Northern Algeria. *Sed Geol* 156:213–239
- Building Seismic Safety Council (BSSC) (2000) The 2000 NEHRP recommended provisions for new buildings and other structures, part I (provisions) and part II (commentary). FEMA 368/369, Washington, D.C
- CEN (2004) Eurocode 8, design of structures for earthquake resistance—part 1: general rules, seismic actions and rules for buildings. EN 1998-1: 2004. Comité Européen de Normalisation, Brussels
- Chiou B, Youngs R, Abrahamson N, Addo K (2010) Ground-motion attenuation model for small-to-moderate shallow crustal earthquakes in California and its implications on regionalization of ground-motion prediction models. *Earthq Spectra* 26:907–926
- Di Alessandro C, Bonilla LB, Boore DM, Rovelli A, Scotti O (2012) Predominant period site classification for response spectra prediction equations in Italy. *Bull Seismol Soc Am* 102(2):680–695
- Douglas J, Boore DM (2011) High-frequency filtering of strong-motion records. *Bull Earthq Eng* 9:395–409. <https://doi.org/10.1007/s10518-010-9208-4>
- Frisenda M, Massa M, Spallarossa D, Ferretti G, Eva C (2005) Attenuation relationship for low magnitude earthquakes using standard seismometric records. *J Earthq Eng* 9:23–40
- Fukushima Y (1997) Comment on ground motion attenuation relation for subduction zones. *Seismol Res Lett* 68:947–949
- Fukushima Y, Tanaka T (1990) A new attenuation relation for peak horizontal acceleration of strong earthquake in Japan. *Bull Seismol Soc Am* 80:757–783
- Fukushima Y, Tanaka T (1992) Revised attenuation relation of peak horizontal acceleration by using a new data base. *Programme Abstr Seismol Soc Jpn* 2:116

- Fukushima Y, Irikura K, Uetake T, Matsumoto H (2000) Characteristics of observed peak amplitude for strong ground motion from the 1995 Hyogo-ken Nanbu (Kobe) earthquake. *Bull Seismol Soc Am* 90:545–565
- Fukushima Y, Berge-Thierry C, Volant P, Griot Pommera DA, Cotton F (2003) Attenuation relation for west Eurasia determined with recent near fault records from California, Japan and Turkey. *J Earthq Eng* 7:573–598
- Fukushima Y, Bonilla LF, Scotti O, Douglas J (2007) Site classification using horizontal to vertical response spectral ratios and its impact when deriving empirical ground motion prediction equations. *J Earthq Eng* 11:712–724
- Ghasemi H, Zare M, Fukushima Y, Sinaeian F (2009) Applying empirical method in site classification, using response spectral ratio (H/V). A case study on Iranian strong motion network (ISMN). *Soil Dyn Earthq Eng* 29:121–132
- Gherboudj F, Laouami N (2013) Scalar and vector probabilistic seismic hazard analysis: application for Algiers City. *J Seismol*. <https://doi.org/10.1007/s10950-013-9380-5>
- Joyner WB, Boore DM (1981) Peak horizontal acceleration and velocity from strong-motion records including records from the 1979 Imperial Valley, California, earthquake. *Bull Seismol Soc Am* 71:2011–2038
- Kawase H, Sanchez-Sesma FJ, Matsushima S (2011) The optimal use of horizontal to vertical ratios of earthquake motions for velocity inversions based on diffuse field theory for plane waves. *Bull Seismol Soc Am* 101:2001–2014
- Kinematics (1989) SSA-1 model, transitory recorded accelerograph. User's manual. Kinematics/Systems Doc 301513 E, Pasadena, California
- Kinematics (1997) SMA Scanview PlusTM: scanner-based software for film accelerogram digitization. User's guide. Kinematics/Systems, Pasadena, California, p 56
- Kinematics (2001) Strong motion analyst. User's manual. Kinematics/Systems, Pasadena, California, p 97
- Laouami N, Slimani A (2013) Earthquake induced site effect in the Algiers-boumerdes region: relation between spectral ratios higher peaks and observed damage during the May 21st Mw 6.8 Boumerdes. *Pure Appl Geophys* 170:1785–1801. <https://doi.org/10.1007/s00024-012-0612-3>
- Laouami N, Slimani A, Bouhadad Y, Chatelain JL, Nour A (2006) Evidence for fault-related directionality and localized site effects from strong motion recordings of the 2003 Boumerdes (Algeria) earthquake: consequences on damage distribution and the Algerian seismic code. *Soil Dyn Earthq Eng* 26:991–1003
- Liu KS, Tsai YB (2005) Attenuation relationships for peak ground acceleration and velocity for crustal earthquakes in Taiwan. *Bull Seismol Soc Am* 95:1045–1058. <https://doi.org/10.1785/0120040162>
- Massa M, Marzorati S, D'Alema E, Di Giacomo D, Augliera P (2007) Site classification assessment for estimating empirical attenuation relationships for central northern Italy earthquakes. *J Earthq Eng* 11:943–967
- RPA (2003) Règlement Parasismique Algérien. CGS Earthquake Engineering Research Center, Rue Kadour Rahim, BP 252, Hussein Dey, Algiers, Algeria
- Sabetta F, Lucantoni A, Bungum H, Bommer J (2005) Sensitivity of PSHA results to ground motion prediction relations and logic-tree weights. *Soil Dyn Earthq Eng* 25:317–329. <https://doi.org/10.1016/j.soildyn.2005.02.002>
- Sadigh K, Chang CY, Egan JA, Makdisi F, Young RR (1997) Attenuation relationships for shallow crustal earthquakes based on California strong motion data. *Seismol Res Lett* 68:180–189
- Skarlatoudis AA, Papazachos CB, Margaris BN (2002) Determination of noise spectra from strong motion data recorded in Greece. In: 12th European conference on earthquake engineering, Paper reference 384, p 10
- Spudich P, Fletcher JB, Hellweg M, Boatwright J, Sullivan C, Joyner WB, Hanks TC, Boore DM, McGarr A, Baker LM, Lindh AG (1997) SEA96—a new predictive relation for earthquake ground motion in extensional tectonic regimes. *Seismol Res Lett* 68:190–198
- Trifunac MD (1976) Preliminary empirical model for scaling Fourier amplitude spectra of strong ground acceleration in terms of earthquake magnitude, source to station distance and recording site conditions. *Bull Seismol Soc Am* 66:1343–1373
- Trifunac MD, Udawadia FE, Brady AG (1973) Analysis of errors in digitized strong motion accelerograms. *Bull Seismol Soc Am* 63:157–187
- Yamazaki F, Ansary MA (1997) Horizontal-to-vertical spectrum ratio of earthquake ground motion for site characterization. *Earthq Eng Struct Dyn* 26:671–689
- Zhao JX, Irikura K, Zhang J, Fukushima Y, Somerville PG, Asano A et al (2006) An empirical site-classification method for strong strong-motion stations in Japan using H/V response spectral ratio. *Bull Seismol Soc Am* 96:914–925